PHYSICAL REVIEW B **80**, 140510(R) (2009)

Electronic structure of $Pr_{2-x}Ce_xCuO_4$ studied via ARPES and LDA+DMFT+Σ_k

I. A. Nekrasov, N. S. Pavlov, E. Z. Kuchinskii, and M. V. Sadovskii
Institute for Electrophysics, Russian Academy of Sciences, Ekaterinburg 620016, Russia

Z. V. Pchelkina
Institute for Metal Physics, Russian Academy of Sciences, Ekaterinburg 620219, Russia

V. B. Zabolotnyy, J. Geck, B. Büchner, and S. V. Borisenko
Institute for Solid State Research, IFW-Dresden, P.O. Box 270116, D-01171 Dresden, Germany

D. S. Inosov
Max-Planck-Institute for Solid State Research, Heisenbergstrasse 1, D-70569 Stuttgart, Germany
and Institute for Solid State Research, IFW-Dresden, P.O. Box 270116, D-01171 Dresden, Germany

A. A. Kordyuk
Institute for Solid State Research, IFW-Dresden, P.O. Box 270116, D-01171 Dresden, Germany
and Institute of Metal Physics of National Academy of Sciences of Ukraine, 03142 Kyiv, Ukraine

M. Lambacher and A. Erb
Walther-Meißner-Institut, Bayerische Akademie der Wissenschaften, Walther-Meißner Strasse 8, 85748 Garching, Germany
(Received 24 June 2009; revised manuscript received 19 August 2009; published 22 October 2009)

The electron-doped $Pr_{2-x}Ce_xCuO_4$ (PCCO) compound in the pseudogap regime ($x \approx 0.15$) was investigated using the angle-resolved photoemission spectroscopy and the generalized dynamical mean-field theory (DMFT) with the **k**-dependent self-energy (LDA+DMFT+Σ_k). Model parameters (hopping integral values and local Coulomb interaction strength) for the effective one-band Hubbard model were calculated by the local-density approximation (LDA) with numerical renormalization-group method employed as an "impurity solver" in DMFT computations. An "external" **k**-dependent self-energy Σ_k was used to describe interaction of correlated conducting electrons with short-range antiferromagnetic (AFM) pseudogap fluctuations. Both experimental and theoretical spectral functions and Fermi surfaces were obtained and compared demonstrating a good semiquantitative agreement. For both experiment and theory normal-state spectra of nearly optimally doped PCCO show clear evidence for a pseudogap state with AFM-like nature. Namely, folding of quasiparticle bands as well as the presence of the "hot spots" and "Fermi arcs" was observed.

DOI: 10.1103/PhysRevB.80.140510 PACS number(s): 74.72.−h, 74.20.−z, 74.25.Jb, 31.15.A−

I. INTRODUCTION

Many experimental and theoretical papers have been seeking to describe the nature of high-temperature superconductivity (HTSC) in cuprates. In contrast to the normal (Fermi-liquid) metal, HTSC compounds show many abnormal properties for temperatures above the superconducting transition, with the normal-state pseudogap being a noted example.[1] The origin of this anomalous state is usually attributed either to superconducting fluctuations (precursor Cooper pairing)[2] or to some order parameters competing with superconductivity,[3,4] e.g., antiferromagnetic (AFM) fluctuations, incommensurate or fluctuating charge-density waves (CDWs), stripes, etc.

Recently a generalized LDA+DMFT+Σ_k computational scheme was proposed to describe the pseudogap state in strongly correlated systems, by accounting for nonlocal AFM (or CDW) fluctuations with short-range order.[5–7] Its relation to other theoretical dynamical mean-field theory (DMFT)-like[8] approaches to the pseudogap state was discussed, e.g., in Ref. 4. Both model computations and those for real systems were done.[4,9] This approach, for instance, allowed one to describe the experimentally observed partial Fermi-surface (FS) "destruction,"[5] which was theoretically studied for hole-doped HTSC prototype system $Bi_2Sr_2CaCu_2O_{8-\delta}$ (Bi2212) (Ref. 4) and electron-doped one $Nd_{1.85}Ce_{0.15}CuO_4$ (NCCO).[9] Two-particle properties can also be described by this approach,[7] e.g., calculated optical spectra in the pseudogap state compare well with experimental data for Bi2212 (Ref. 4) and NCCO (Ref. 9).

In this Rapid Communication we study the electron-doped $Pr_{2-x}Ce_xCuO_4$ (PCCO) in the pseudogap state ($x=0.15$) using the generalized LDA+DMFT+Σ_k computational scheme[5–7] and angle-resolved photoemission spectroscopy (ARPES) measurements.[10,11] We present here both experimental and theoretical quasiparticle spectral functions and Fermi surfaces. These are found to agree well with each other supporting competing order parameter fluctuations as the origin of the pseudogap instead of the superconducting scenario.

II. COMPUTATIONAL DETAILS

The crystal structure[12] of Pr_2CuO_4 has tetragonal symmetry and the space group is $I4/mmm$. The lattice constants[12]

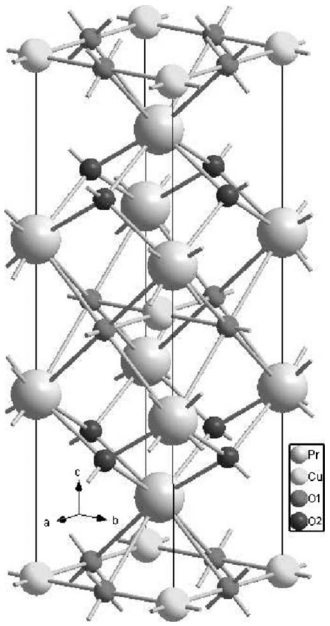

FIG. 1. The crystal structure of Pr_2CuO_4. Medium size gray spheres correspond to the copper atoms, small dark and black spheres are O1 and O2 atoms, respectively, and big gray spheres correspond to praseodymium atoms.

are $a=b=3.962$ and $c=12.154$ Å. There are two crystallographic types of oxygen atoms in Pr_2CuO_4: the first one belongs to CuO_2 layer and the second is located within the Pr atoms. The atomic positions in the elementary cell are as follows: Cu, $2a(0,0,0)$; O1, $4c(0,0.5,0)$; Pr, $4e(0,0,0.35171)$; and O2, $4d(0,0.5,0.25)$.[12]

In Fig. 1 the crystal structure of Pr_2CuO_4 is shown. Medium size gray spheres correspond to the copper atoms, small dark and black spheres represent O1 and O2 atoms, and big gray spheres show praseodymium positions. Clearly visible quasi-two-dimensional nature of these compounds determines its physical properties. Physically most interesting are the CuO_2 layers. Those layers provide antibonding Cu-$3d(x^2-y^2)$ partially filled orbital, whose dispersion crosses the Fermi level (FL). Thus, we are using this effective Cu-$3d(x^2-y^2)$ antibonding band as a "bare" band in DMFT computations.

The electronic structure of PCCO was investigated within generalized LDA+DMFT+$\Sigma_{\mathbf{k}}$ scheme.[5–7] This scheme incorporates the density-functional theory in local-density approximation (LDA) (Ref. 13) and the DMFT (Ref. 8) with external momentum-dependent self-energy $\Sigma_{\mathbf{k}}$.[6]

As a first step the LDA band-structure calculation was performed. Using crystal structure data, the electronic band structure was obtained with the linearized muffin-tin orbital (LMTO) method.[14] Further hopping integral values were calculated for the effective Cu-$3d(x^2-y^2)$ Wannier function within the Nth-order LMTO framework.[15] The corresponding hopping integral values are $t=-0.4385$, $t'=0.1562$, and $t''=0.0976$. The value of Coulomb interaction on effective Cu-$3d(x^2-y^2)$ orbital $U=1.1$ eV was obtained via constrained LDA computations.[16] Second, the DMFT calculations,[8] which take the hopping integrals and the Coulomb interaction as input parameters, were performed.

To account for the AFM spin fluctuations, a two-dimensional model of the pseudogap state is applied.[17] The corresponding $\mathbf{k}$-dependent self-energy $\Sigma_{\mathbf{k}}$ (Refs. 1 and 17) describes nonlocal correlations induced by (quasi)static short-range collective Heisenberg-like AFM spin fluctuations. The quasistatic approximation for AFM fluctuations necessarily limits our approach to high-enough temperatures (energies not so close to the Fermi level),[17] so that in fact we are unable to judge, e.g., on the nature of low-temperature (-energy) damping in our model. Thus, we avoid here possible discussion of whether the damping corresponds to marginal or regular Fermi liquid. Moreover, as shown in Ref. 6 for the hot spot the corresponding self-energy has essentially non-Fermi-liquid behavior.

The $\Sigma_{\mathbf{k}}$ definition contains two important parameters: the pseudogap energy scale (amplitude) Δ, representing the energy scale of fluctuating spin density waves (SDW), and the spatial correlation length ξ. The latter is usually determined from experiment. The Δ value was calculated as described in Ref. 6 and found to be 0.275 eV. The value of correlation length was taken to be 50 lattice constants, in accordance with the typical value obtained in neutron scattering experiments on NCCO.[18] To solve DMFT equations numerical renormalization group (NRG) (Refs. 19 and 20) was employed as an impurity solver. The corresponding temperature of DMFT (NRG) computations was 0.011 eV and the electron concentration was $n=1.145$.

III. EXPERIMENTAL DETAILS

Photoemission experiments were performed at UE112-PGM beamline at BESSY using SCIENTA SES100 analyzer. The typical energy and the angular resolution for the excitation energy ($h\nu=100$ eV) used in this study were 20 meV and 0.2°, respectively. Samples of $Pr_{1.85}Ce_{0.15}CuO_{4+\delta}$ were grown using traveling solvent floating-zone technique and annealed to achieve an optimal T_c of 25 K with a transition width of 1K, which resulted from improved growth conditions.[21] Similarly the width (full width at half maximum) of x-ray rocking curves was less than 0.08°, signaling high quality of the samples.

For the photoemission measurements the samples were mounted on a cryomanipulator and cleaved *in situ* in ultrahigh vacuum with a base pressure of $\lesssim 1\times 10^{-10}$ mbar. During the whole experiment, including the temperature cycling, when the sample was heated to room temperature and then cooled back again, no observable aging effects were detected.

IV. RESULTS AND DISCUSSION

Generally speaking, finite temperature and interaction lead to notable lifetime effects. Thus, instead of quasiparticle dispersions obtained in usual band-structure calculations one has to deal with the corresponding spectral function $A(\omega,\mathbf{k})$,

$$A(\omega,\mathbf{k}) = -\frac{1}{\pi}\mathrm{Im}\, G(\omega,\mathbf{k}), \tag{1}$$

where $G(\omega,\mathbf{k})$ is the retarded Green's function obtained via the LDA+DMFT+$\Sigma_{\mathbf{k}}$ scheme.[5–7]

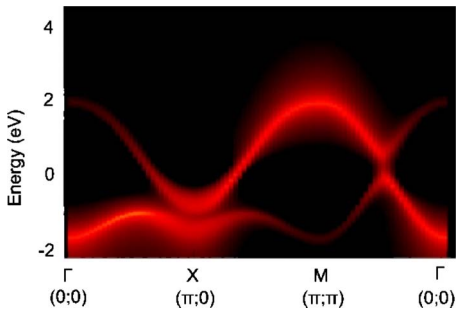

FIG. 2. (Color online) LDA+DMFT+$\Sigma_{\mathbf{k}}$ quasiparticle energy dispersion of PCCO Cu-$3d(x^2-y^2)$ orbital for high symmetry directions of square Brillouin zone. The Fermi level is zero. Here and below intensity goes down as yellow-red-black.

Color plots, whose intensity encodes the function values, became a traditional and convenient way of representing these multiple variable functions. Such a color plot of LDA+DMFT+$\Sigma_{\mathbf{k}}$ quasiparticle spectral function (1) of copper $3d(x^2-y^2)$ orbital is presented in Fig. 2. The width of the quasiparticle spectral function in the color plot is inversely proportional to the quasiparticle lifetime. The calculated quasiparticle band dispersion has a minimum at Γ point (−1.52 eV) and a maximum at *M* point (2 eV). It crosses the Fermi level along *X*-*M* as well as *M*-Γ directions. Because of AFM pseudogap fluctuations there is a well detectable (quasi)folding of the quasiparticle band, reflected in the formation of the so-called "shadow" band, which has its maxima at Γ point and minima at *M* point. However, because of the short-range nature of the antiferromagnetic order, this does not result in a complete folding, as it would be the case for a long-range AFM order. Namely, quasiparticle band and the shadow band are not exactly the same. No real band gap opens at $(\pi/2,\pi/2)$ point. Nevertheless, the suppression of the spectral weight is clearly detectable in the vicinity of *X* $(\pi,0)$ point, thus signaling opening of the pseudogap, which in this case can be viewed as a precursor of the real band gap. Splitting takes place between the quasiparticle band and the shadow band with the value of about 2Δ.

In Fig. 3 an extended picture of PCCO Fermi surfaces is presented [Fig. 3(a): LDA+DMFT+$\Sigma_{\mathbf{k}}$ results; Fig. 3(b): experimental ARPES data]. Strictly speaking Fig. 3 is a color

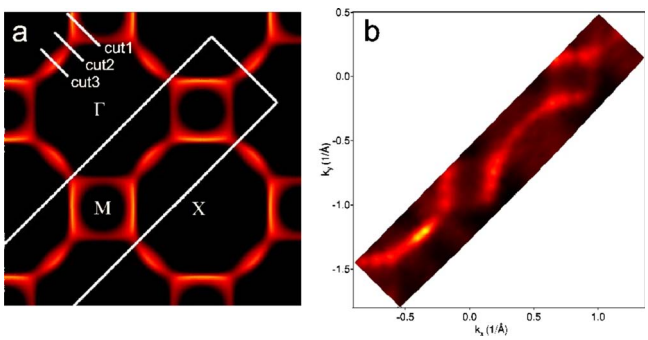

FIG. 3. (Color online) (a) Extended Fermi surfaces for PCCO-LDA+DMFT+$\Sigma_{\mathbf{k}}$ data. White rectangle in (a) schematically shows the part of reciprocal space measured experimentally (b). Lower left corner is *X* point $(\pi,0)$.

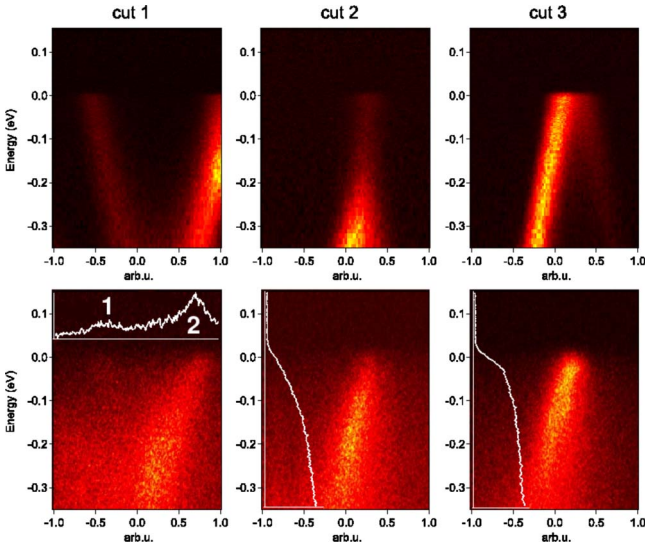

FIG. 4. (Color online) Energy-momentum intensity distributions for the specific cuts drawn in Fig. 3 (upper panels: theoretical data; lower panels: experimental photoemission intensity). To judge about the absolute intensities of the shadow (1) and main band (2), cut 1 contains momentum distribution curves (MDC) integrated in an energy window of 60 meV centered at the FL. Similarly, integral energy distribution curves (EDC) for cut 2 (hot spot) show suppression of the intensity at the FL as compared to cut 3, which is located further away from the hot spot. The FL is zero.

map in reciprocal space of the corresponding spectral function plotted at the Fermi level. FS is clearly visible as reminiscence of noninteracting band close to the first Brillouin-zone border and around $(\pi/2,\pi/2)$ point (the so-called Fermi arc), where the quasiparticle band crosses the Fermi level. There is an interesting physical effect of partial destruction of the FS observed in the hot spots: points that are located at the intersection of the FS and its AFM umklapp replica. This FS destruction occurs because of the strong electron scattering on the AFM spin (pseudogap) fluctuations on the copper atoms. Also the shadow FS is visible as it should be for AFM folding. As no long-range order is present in the underdoped phase the shadow FS has a weaker intensity with respect to FS. Another evidence of the presence of electron pockets can be seen in the experimental FS map shown in Fig. 3(b). One pocket is centered at a point with coordinates $(0,0.8\pi)$ and the other at $(0.8\pi,0)$. Again, in agreement with the theoretical prediction, the pocket "sides" that coincide with originally unreconstructed FS have higher intensity, while the newly appearing "replicas" or shadows have weaker intensity.

The PCCO FS is very similar to that of $Nd_{2-x}Ce_xCuO_4$, which belongs to the same family of superconductors. The NCCO was recently studied both theoretically[9] and experimentally.[22]

Let us compare theoretical (upper line) and experimental (lower line) energy quasiparticle dispersions for most characteristic cuts introduced in Fig. 3 (see Fig. 4). Theoretical data were multiplied by the Fermi function at a temperature of 30 K and convoluted with a Gaussian to simulate the effects of experimental resolution, with further artificial noise added.

Cut 1 intersects quasiparticle and shadow Fermi surfaces close to the Brillouin-zone border. One can find here a "fork-like" structure formed by the damped shadow band [−0.5–0 arbitrary units (a.u.)] and better defined quasiparticle band (0.5–1 a.u.). This structure corresponds to the preformation of FS cylinder around $(\pi,0)$ point. Cut 2 goes exactly through the hot spot. Here, we see a strong suppression of the quasiparticle band around the Fermi level as it is also shown in Fig. 2. Cut 3 crosses the Fermi arc, where we can see a very well defined quasiparticle band. However, weak intensity shadow band is also present. For the case of long-range AFM order and complete folding of electronic structure, FS and its shadow should form a closed FS sheet around $(\pi/2,\pi/2)$ point, while in the current case the part of the pocket formed by the shadow band is not so well defined in the momentum space. As can be seen there is a good correspondence between the calculated and the experimental data in terms of the above described behavior, which is also similar to the results reported for $Nd_{2-x}Ce_xCuO_4$ in our earlier work.[9]

V. CONCLUSION

In this work the LDA+DMFT+$\Sigma_{\mathbf{k}}$ was performed for electron-doped $Pr_{2-x}Ce_xCuO_4$ compound in the pseudogap regime. The LDA+DMFT+$\Sigma_{\mathbf{k}}$ calculation shows that Fermi-liquid behavior is still conserved far away from the hot spots, while the destruction of the Fermi surface observed in the vicinity of hot spots is due to the strong scattering of correlated electrons on short-range antiferromagnetic (pseudogap) fluctuations. Comparison between experimental ARPES and LDA+DMFT+$\Sigma_{\mathbf{k}}$ data reveals a good semiquantitative agreement. The experimental and theoretical results obtained once again support the AFM scenario of pseudogap formation not only in hole-doped HTSC systems[4] but also in electron-doped ones.[9]

ACKNOWLEDGMENTS

We thank Thomas Pruschke for providing us the NRG code. This work was supported by RFBR Grants No. 08-02-00021 and No. 08-02-91200 and RAS programs "quantum physics of condensed matter" and "strongly correlated electrons in solids." I.A.N. and Z.V.P. are supported by Grants of President of Russia No. MK-3227.2008.2 (Z.V.P.) and No. MK-614.2009.2 (I.A.N.), Russian Science Support Foundation (I.A.N.), and the Dynasty Foundation (Z.V.P.). The experimental measurements for this study were possible owing to the financial support of Forschergruppe Grant No. FOR538 and by the DFG under Grant No. KN393/4.

[1] T. Timusk and B. Statt, Rep. Prog. Phys. **62**, 61 (1999); M. V. Sadovskii, Phys. Usp. **44**, 515 (2001); M. V. Sadovskii, in "Strings, branes, lattices, networks, pseudogaps and dust" (Proc. I. E. Tamm seminar) (Scientific World, Moscow, 2007), pp. 357–441 (in Russian), English version arXiv:cond-mat/0408489 (unpublished).

[2] V. J. Emery and S. A. Kivelson, Nature (London) **374**, 434 (1995).

[3] A. A. Kordyuk, S. V. Borisenko, V. B. Zabolotnyy, R. Schuster, D. S. Inosov, D. V. Evtushinsky, A. I. Plyushchay, R. Follath, A. Varykhalov, L. Patthey, and H. Berger, Phys. Rev. B **79**, 020504(R) (2009).

[4] E. Z. Kuchinskii, I. A. Nekrasov, Z. I. Pchelkina, and M. V. Sadovskii, JETP **104**, 792 (2007); I. A. Nekrasov, E. Z. Kuchinskii, Z. V. Pchelkina, and M. V. Sadovskii, Physica C **460-462**, 997 (2007).

[5] E. Z. Kuchinskii, I. A. Nekrasov, and M. V. Sadovskii, JETP Lett. **82**, 198 (2005).

[6] M. V. Sadovskii, I. A. Nekrasov, E. Z. Kuchinskii, Th. Pruschke, and V. I. Anisimov, Phys. Rev. B **72**, 155105 (2005).

[7] E. Z. Kuchinskii, I. A. Nekrasov, and M. V. Sadovskii, Phys. Rev. B **75**, 115102 (2007).

[8] A. Georges, G. Kotliar, W. Krauth, and M. J. Rozenberg, Rev. Mod. Phys. **68**, 13 (1996).

[9] E. E. Kokorina, E. Z. Kuchinskii, I. A. Nekrasov, Z. V. Pchelkina, M. V. Sadovskii, A. Sekiyama, S. Suga, and M. Tsunekawa, JETP **107**, 828 (2008); I. A. Nekrasov *et al.*, J. Phys. Chem. Solids **69**, 3269 (2008).

[10] A. Damascelli, Z. Hussain, and Zhi-Xun Shen, Rev. Mod. Phys. **75**, 473 (2003).

[11] A. A. Kordyuk and S. V. Borisenko, Low Temp. Phys. **32**, 298 (2006).

[12] D. E. Cox, A. I. Goldman, M. A. Subramanian, J. Gopalakrishnan, and A. W. Sleight, Phys. Rev. B **40**, 6998 (1989).

[13] R. O. Jones and O. Gunnarsson, Rev. Mod. Phys. **61**, 689 (1989).

[14] O. K. Andersen, Phys. Rev. B **12**, 3060 (1975); O. K. Andersen and O. Jepsen, Phys. Rev. Lett. **53**, 2571 (1984).

[15] O. K. Andersen and T. Saha-Dasgupta, Phys. Rev. B **62**, R16219 (2000); O. K. Andersen *et al.*, Psi-k Newsletter **45**, 86 (2001); O. K. Andersen, T. Saha-Dasgupta, and S. Ezhov, Bull. Mater. Sci. **26**, 19 (2003).

[16] O. Gunnarsson, O. K. Andersen, O. Jepsen, and J. Zaanen, Phys. Rev. B **39**, 1708 (1989).

[17] J. Schmalian, D. Pines, and B. Stojkovic, Phys. Rev. B **60**, 667 (1999); É. Z. Kuchinskii and M. V. Sadovskii, JETP **88**, 968 (1999).

[18] I. A. Zobkalo *et al.*, Solid State Commun. **80**, 921 (1991); E. M. Motoyama, G. Yu, I. M. Vishik, O. P. Vajk, P. K. Mang, and M. Greven, Nature (London) **445**, 186 (2007).

[19] K. G. Wilson, Rev. Mod. Phys. **47**, 773 (1975); H. R. Krishna-Murthy, J. W. Wilkins, and K. G. Wilson, Phys. Rev. B **21**, 1003 (1980); **21**, 1044 (1980).

[20] R. Bulla, A. C. Hewson, and Th. Pruschke, J. Phys.: Condens. Matter **10**, 8365 (1998).

[21] M. Lambacher, Ph.D. thesis, Technische Universität München, 2008.

[22] N. P. Armitage, F. Ronning, D. H. Lu, C. Kim, A. Damascelli, K. M. Shen, D. L. Feng, H. Eisaki, Z.-X. Shen, P. K. Mang, N. Kaneko, M. Greven, Y. Onose, Y. Taguchi, and Y. Tokura, Phys. Rev. Lett. **88**, 257001 (2002).